Reconstructing a complex field from a series of its near-field diffraction patterns*

Hong You-Li(洪友丽)[a)], Zhang Kai(张 凯)[a)], Wang Zhi-Li(王志立)[b)], Zhu Zhong-Zhu(朱中柱)[a)], Zhao Xue-Jiao(赵雪娇)[a)], Huang Wan-Xia(黄万霞)[a)], Yuan Qing-Xi(袁清习)[a)], Zhu Pei-Ping(朱佩平)[a)†], and Wu Zi-Yu(吴自玉)[b)a)‡]

[a)] *Beijing Synchrotron Radiation Facility, Institute of High Energy Physics, Chinese Academy of Sciences, Beijing* 100049, *China*

[b)] *National Synchrotron Radiation Laboratory, University of Science and Technology of China, Hefei* 230026, *China*

(Received 5 February 2012; revised manuscript received 15 February 2012)

We propose a method for reconstructing a complex field from a series of its near-field diffraction patterns. This method is based on the paraxial Fresnel diffraction equation without making further approximations. Numerical simulations are presented showing that a complex field can even be reconstructed with moderate qualities from its two near-field diffraction patterns and almost exact reconstructions can be obtained when three or more diffraction patterns are used. We also show by numerical simulation that the correct diffraction distances can be recovered in case only coarsely measured values are available. This method may be applied to phase imaging of weak-absorption objects.

Keywords: phase imaging, near field, phase retrieval

PACS: 42.25.Fx, 42.30.Rx **DOI:** 10.1088/1674-1056/21/10/104202

1. Introduction

X-ray phase imaging is an important technique for investigating weak-absorption samples.[1−10] To detect the phase distribution of the X-ray introduced by the sample, one may either use an interferometer[11,12] or let the X-ray wave propagate to certain distances and then try to extract the phase information from the diffraction patterns. The process is usually called phase retrieval or phase recovery.[13] When the Fresnel number is not too big (it is usually limited to several tens or smaller), Fraunhofer coherent diffraction imaging (CDI)[14−17] or the Fresnel CDI method[18−21] can be used to reconstruct the object field from a single diffraction pattern. However, when the Fresnel numbers are bigger in the case of near-field diffraction imaging of larger objects, it is usually difficult to perform Fraunhofer or Fresnel CDI.[22] Various methods for this problem have been developed. For phase retrieval from a single near-field diffraction pattern one may use the algorithms developed by Cheng *et al.*,[23,24] where weak phase object approximation is used, or those by Li *et al.*,[22,25] which deal with the more general cases but requires oversampling of the diffraction pattern. For phase retrieval from multiple near-field diffraction patterns, both linear and nonlinear ones are available. Since multiple diffraction patterns are used, oversampling is not required in any of these methods. Linear methods may include the transport-of-intensity equation method (TIE),[26−31] the astigmatic imaging method,[32] the composite linear method,[33] and the holography method.[34] The linear methods are easy to solve and have had many successful applications but in principle they assume weak phase objects or/and slow phase variation in order to drop the nonlinear terms in the equations. The nonlinear methods have no such limitations. Allen *et al.* demonstrated that by iteratively propagating the waves between the object and diffraction planes and applying the diffraction intensity constraints one can reconstruct the object field from three or more diffraction patterns.[35,36] Zhang *et al.* demonstrated a phase retrieval method that an arbitrary com-

*Project supported by the National Basic Research Program of China (Grant Nos. 2012CB825800 and 2009CB930804), the Key Important Project of the National Natural Science Foundation of China (Grant No. 10734070), the National Natural Science Foundation of China (Grant Nos. 11179004 and 10979055), and the Knowledge Innovation Program of the Chinese Academy of Sciences (Grant No. KJCX2-YW-N42).

†Corresponding author. E-mail: zhupp@ihep.ac.cn

‡Corresponding author. E-mail: wuzy@ustc.edu.cn

© 2012 Chinese Physical Society and IOP Publishing Ltd

plex field can be reconstructed from three or more of its Fresnel diffraction patterns collected with an aperture-plane phase plate transversely shifted to different positions.[37] Liu *et al.* proposed a quantitative phase imaging method from its diffraction images using structured illumination.[38] It was also shown that a complex sample can be reconstructed from a series of its de-focused images using polychromatic X-ray illumination.[39]

In this paper we propose an iterative algorithm for directly reconstructing an arbitrary complex field from a series of its near-field diffraction patterns. In the iterations, one does not get the phase distributions of the diffraction fields but simply tries to find optimal object fields to fit the diffraction patterns collected by the pixelated detectors. Compared with other non-linear methods mentioned above, this one has the advantage that the sampling rate need not be great enough to sample the phase of the diffractive fields since one does not use the diffractive fields to propagate them to the object plane or other diffraction plane(s).

The rest of the paper is arranged as follows. Section 2 describes the theory, followed by numerical simulations in Section 3. The conclusion is given in Section 4.

2. Theory

For the sake of simplicity, we only present the theory in the one-dimensional (1D) form, but the extension to the two-dimensional (2D) form is straightforward. Under the paraxial approximation, the object field $E(m;0)$ and the diffraction field $E(p;z)$ at a distance z from the object plane are related by

$$E(p;z)=\sum_{m=-\lfloor N/2\rfloor}^{\lceil N/2\rceil-1}E(m;0)T_z(p-m) \tag{1}$$

with the transfer function $T_z(s)$ defined as

$$T_z(s)=z^{-1/2}\int_{-1/2}^{1/2}\mathrm{d}\alpha\exp\left[\mathrm{i}\pi\left(\frac{N^2}{4N_{\mathrm{F}}}\right)^{-1}(s-\alpha)^2\right]. \tag{2}$$

In the above derivations, we show the sampling interval on the diffraction plane to be the same as that on the object plane. Here $\lfloor x\rfloor$ and $\lceil x\rceil$ denote the floor and ceiling of x, N is the number of object pixels, $\mathrm{i}=(-1)^{1/2}$, $N_{\mathrm{F}}=a^2/(4z\lambda)$ the Fresnel number with λ the wavelength and a the size of the object. Note that while m takes only integer values, p and s can take continuous values. Given that the diffractive intensity $|E(p;z)|^2$ can be effectively measured, one may use Eqs. (1) and (2) to iteratively propagate the wave fields between the object and image planes and apply the diffraction intensity constraints to reconstruct the object. However, practical experiments cannot measure the diffractive intensity at ideal points but integrated intensities over finite-sized pixels. While it is possible to obtain the diffractive intensity at ideal points directly from integrated intensities in the case of far-field diffraction,[40] no similar method has yet been found to exist in the case of near-field diffraction. Indeed, we may expect this effect to be neglected if the sampling of the diffraction pattern is dense enough. However, to do so larger detectors would be needed and the photon counts would be lower. An alternative solution to this problem was demonstrated, that the object may be reconstructed by simply fitting its integrated near-field diffraction intensity to the measured data.[25] In this paper we show that this method also works in the case of reconstructing an object from a series of its near-field diffraction patterns.

To proceed, we denote the number of diffraction images to be N_I, the distances of the diffraction image planes to be z_k, $k=1,\ldots,N_I$, the corresponding transfer functions T_k, then we have

$$E(p;z_k)=\sum_{m=-\lfloor N/2\rfloor}^{\lceil N/2\rceil-1}E(m;0)T_k(p-m). \tag{3}$$

The integrated diffraction intensity collected by pixel q at the distance z_k, denoted by $I^{\exp}(q;z_k)$, is

$$I^{\exp}(q;z_k)=\lim_{L\to+\infty}I(q;z_k;L) \tag{4}$$

with

$$I(q;z_k;L)=\frac{1}{L}\sum_{l=-\lfloor(L-1)/2\rfloor}^{\lceil(L-1)/2\rceil}\left|E\left(\frac{l}{L}+q;z_k\right)\right|^2, \tag{5}$$

where L is an integer. We here define the integrated intensity collected by each pixel to be the limit of averaging the intensities at points within the pixel so that discrete convolution can be used to speed up the calculation as indicated by Eqs. (3) and (5). To reconstruct the object from the measured diffraction intensities, we define the objective function[25]

$$D=\sum_{k=1}^{N_I}\mu_k D_k, \tag{6}$$

where μ_k are real weighting factors and D_k is defined as

$$D_k = \sum_{q=-\lfloor N/2 \rfloor}^{\lceil N/2 \rceil - 1} \left\{ [I(q; z_k; L)]^{1/2} - [I^{\exp}(q; z_k)]^{1/2} \right\}^2. \tag{7}$$

From Eqs. (5)–(7), we see that D is a function of $E(m;0)$ and its minimum corresponds to the solution of the equations

$$\begin{aligned} &\frac{1}{L} \sum_{l=-\lfloor (L-1)/2 \rfloor}^{\lceil (L-1)/2 \rceil} \\ &\times \left| \sum_{m=-\lfloor N/2 \rfloor}^{\lceil N/2 \rceil - 1} E(m;0) T_k \left(\frac{l}{L} + q - m \right) \right|^2 \\ &= I^{\exp}(q; z_k). \end{aligned} \tag{8}$$

If L is sufficiently large, then the solution of Eq. (8) or, equivalently, the minimization of D will converge to the original object function. To minimize D, the following equations can be iteratively applied until convergence is reached[25]

$$E^{(j+1)}(m;0) = E^{(j)}(m;0) - \epsilon G^{(j)}(m), \tag{9}$$

where the superscripts are iteration numbers, ϵ is a real number and has the meaning of the searching step size and $G^{(j)}(m)$ is defined by

$$G^{(j)}(m) = \sum_{k=1}^{N_I} \mu_k G_k^{(j)}(m) \tag{10}$$

with[25]

$$\begin{aligned} G_k^{(j)}(m) = \frac{1}{L} &\sum_{l=-\lfloor (L-1)/2 \rfloor}^{\lceil (L-1)/2 \rceil} \sum_{q=-\lfloor N/2 \rfloor}^{\lceil N/2 \rceil - 1} \Delta^{(j)} \left(\frac{l}{L} + q; z_k \right) \\ &\times T_k^* \left(\frac{l}{L} + q - m \right), \end{aligned} \tag{11}$$

$$\begin{aligned} \Delta^{(j)} \left(\frac{l}{L} + q; z_k \right) = &\left\{ 1 - \left[\frac{I^{\exp}(q; z_k)}{I^{(j)}(q; z_k; L)} \right]^{1/2} \right\} \\ &\times E^{(j)} \left(\frac{l}{L} + q; z_k \right), \end{aligned} \tag{12}$$

where $E^{(j)}(l/L + q; z_k)$ can be calculated from $E^{(j)}(m;0)$ using Eq. (3) and $I^{(j)}(q; z_k; L)$ from $E^{(j)}(l/L + q; z_k)$ using Eq. (5).

3. Numerical simulations

To demonstrate how our method works, we performed numerical simulations. Figures 1(a) and 1(b) show the phase and magnitude distribution of the complex object characterized by 128×128 pixels. Four diffraction images with $N_{\rm F} = 150, 200, 300, 400$ were calculated using Eqs. (2), (4), and (5) from the object zero-padded to a size of 130×130 and it turned out that $I(q; z_k; L)$ converges when $L \geq 1024$. Then Poisson noise was added to the images assuming an average photon count of 400 per pixel for each image and we finally get $I^{\exp}(q; z_k)$ (Figs. 1(c)–1(f)). To reconstruct the object from the diffraction images, the iteration can be carried out simply following Eqs. (9)–(12). In each reconstruction, we started from the initial object $E^{(0)}(m;0) = 1$ and ran the iteration for 1000 cycles with $L = 1$, $\epsilon = 0.02$, and then with $L = 10$, $\epsilon = 0.1$, until convergence was obtained. μ_k was set to be 1 in all cases. To monitor the iteration, the normalized reconstruction error is defined as

$$R^{(j)} = D^{(j)} / \sum_{k=1}^{N_I} \mu_k \sum_q I^{\exp}(q; z_k). \tag{13}$$

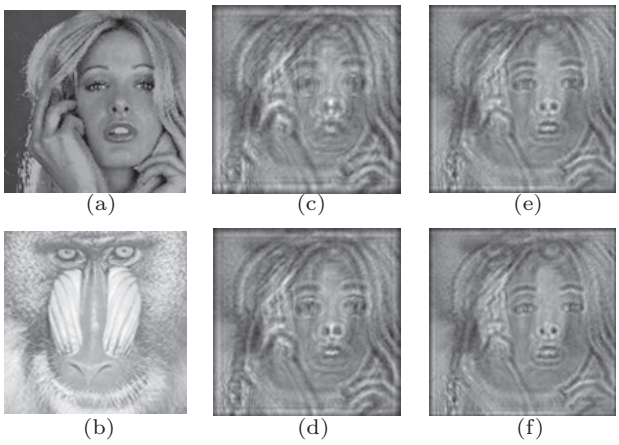


Fig. 1. Panels (a) and (b) show the phase and magnitude distributions of the test object. The phase varies from 0 to π and the magnitude from 0.1 to 1. Panels (c), (d), (e), and (f) show the near-field diffraction magnitudes $[I(q;z)]^{1/2}$ of the object for $N_{\rm F} = 150$, $N_{\rm F} = 200$, $N_{\rm F} = 300$, and $N_{\rm F} = 400$, respectively. Each image has a size of 130×130, the same as the zero-padded object.

In all our simulations, the iterations converged within 5000 steps (Fig. 2). We first used two diffraction images (Figs. 1(d) and 1(f)) and reconstruction with moderate qualities was obtained when the correct Fresnel numbers were used (Figs. 2(a) and 2(b)). We tried different sets of two images and similar results were obtained. When three or four diffraction images were used, the reconstructions were improved as one would expect (Figs. 2(c)–2(f)).

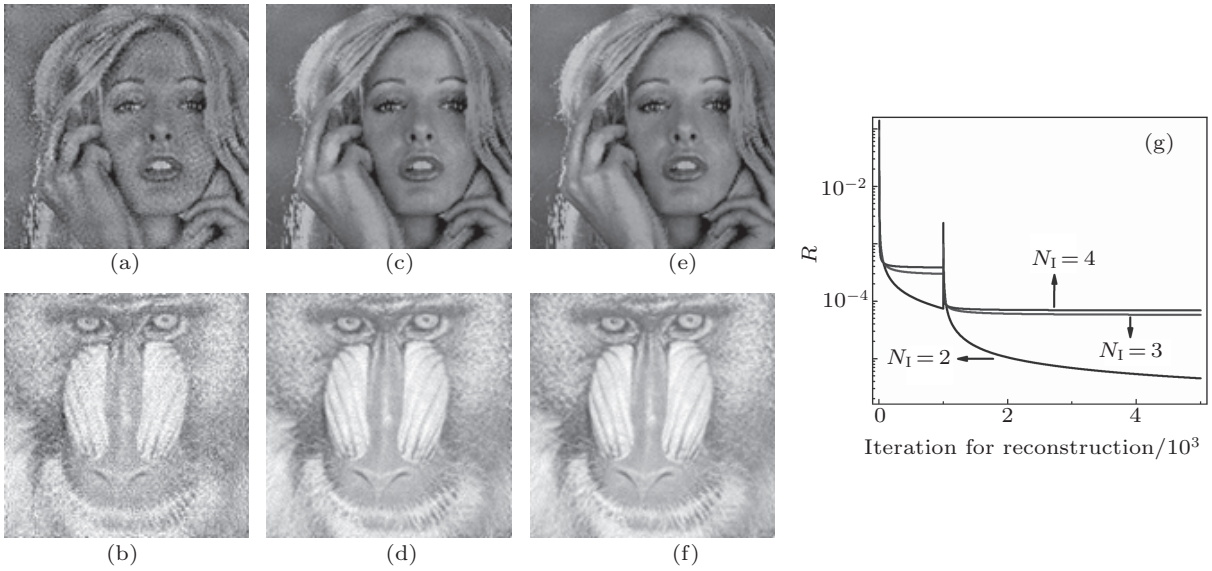


Fig. 2. (colour online) Panels (a) and (b) show the reconstructed phase and magnitude using diffraction images in Figs. 1(d) and 1(f). Panels 2(c) and 2(d) show the reconstructions using Figs. 1(c), 1(d), and 1(f). Panels (e) and (f) show the reconstructions using all the four diffraction images in Figs. 1(c)–1(f). Panel (g) shows the convergence of the normalized reconstruction errors in the reconstruction iterations using the correct Fresnel numbers.

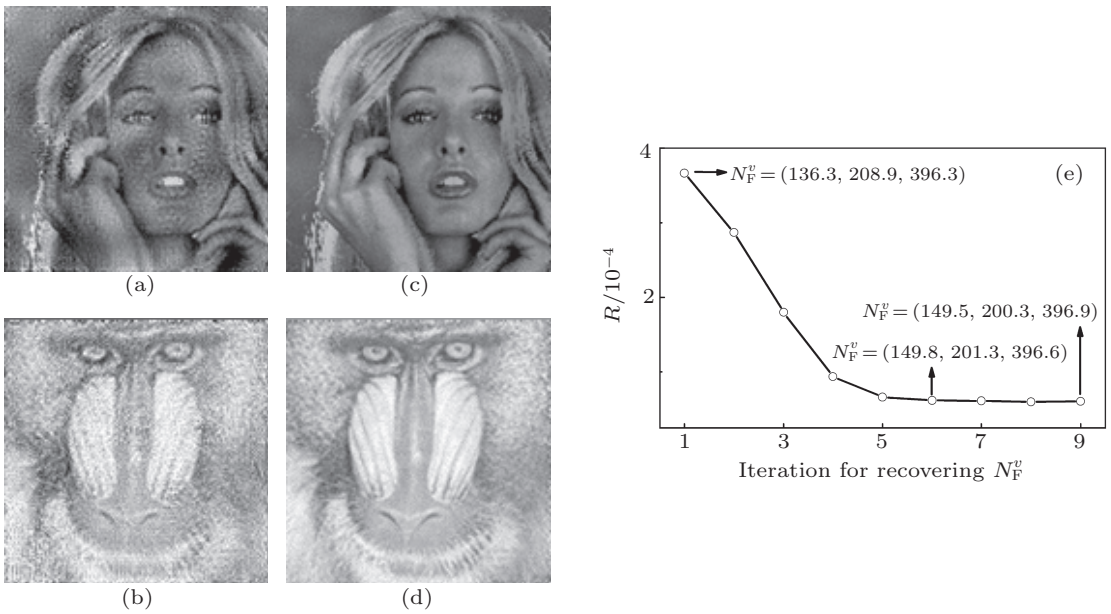


Fig. 3. (colour online) Panels (a), (b), (c), and (d) show the reconstructions using the diffraction images in Figs. 1(c), 1(d), and 1(f) using incorrect and recovered Fresnel numbers, respectively. Panel (e) shows the convergence of the iteration retrieving the correct Fresnel numbers. The iteration starts with the incorrect Fresnel numbers $\boldsymbol{N}_{\rm F}^v = (136.3, 208.9, 396.3)$ and converges at $\boldsymbol{N}_{\rm F}^v = (149.5, 200.3, 396.9)$.

Since the Fresnel numbers may not be accurately measured in practical experiments, it is important that the algorithm can deal with such measurement errors. We developed an efficient method that recovers the correct Fresnel numbers from coarsely measured values. We denote the Fresnel numbers used in the reconstructions by a vector $\boldsymbol{N}_{\rm F}^v = (\ldots, N_{{\rm F},k}, \ldots)$, where $k = 1, \ldots, N_I$. Once we have an estimate of $\boldsymbol{N}_{\rm F}^v$, we perform reconstructions following the steps described above using the Fresnel numbers of $\boldsymbol{N}_{\rm F}^v$ and $\boldsymbol{N}_{{\rm F},k}^v = (\ldots, N_{{\rm F},(k-1)}, N_{{\rm F},k}+1, N_{{\rm F},(k+1)} \ldots)$ getting a normalized reconstruction error of R and R_k. We define $g_k = R_k - R$. Obtaining g_k for $k = 1, \ldots, N_I$, a new estimate of the Fresnel numbers can be calcu-

lated as $\boldsymbol{N}_{\mathrm{F}}^{v'} = \boldsymbol{N}_{\mathrm{F}}^{v} - (\ldots, g_k, \ldots) \cdot \tau$, with τ being a real number. This procedure can be carried out until convergence is reached. We tested this approach using a set of three diffraction images (Figs. 1(c), 1(d), and 1(f)). The iteration started with a set of randomly generated Fresnel numbers $\boldsymbol{N}_{\mathrm{F}}^{v} = (136.3, 208.9, 396.3)$ with an average deviation of about 5% from the correct values and $\tau = 6 \times 10^4$, and it converged within 9 loops arriving at $\boldsymbol{N}_{\mathrm{F}}^{v} = (149.5, 200.3, 396.9)$, as indicated in Fig. 3(e). As shown in Fig. 3(a)–3(d), the reconstructions are much improved when the recovered Fresnel numbers are used. Numerical simulations were also carried out with different sets of randomly generated Fresnel numbers and different sets of images, and correct Fresnel numbers were recovered in all these tests.

4. Conclusion

In conclusion we have developed a method for reconstructing a complex field from a series of its near-field diffraction images. We showed by numerical simulation that moderate reconstructions can be obtained with even two diffraction images and almost exact reconstructions can be obtained when three or four diffraction images are used. We also showed that even if the accurate values of the Fresnel numbers are not known, they can still be recovered using an efficient algorithm. Although the algorithm seems efficient and robust, we do note that there are still very challenging and important questions such as the uniqueness of problem and the convergence property of the algorithm to be answered.

References

[1] Davis T J, Gao D, Gureyev T E, Stevenson A W and Wilkins S W 1995 *Nature* **373** 595

[2] Gao D C, Pogany A, Stevenson A W, Gureyev T, Wilkins S W and Mai Z 2000 *Acta Phys. Sin.* **49** 2357 (in Chinese)

[3] Huang W X, Tian Y L, Zhu P P, Mai Z H and Hu X F 2002 *Acta Phys. Sin.* **51** 1040 (in Chinese)

[4] Hwu Y, Tsai W, Je J, Seol S, Kim B, Groso A, Margaritondo G, Lee K and Seong J 2004 *Phys. Med. Biol.* **49** 501

[5] Chen M, Xiao T Q, Luo Y Y, Lu L X, Wei X, Du G H and Xu H J 2004 *Acta Phys. Sin.* **53** 2953 (in Chinese)

[6] Liu L X, Du G H, Hu W, Luo Y Y, Xie H L, Chen M and Xiao T Q 2006 *Acta Phys. Sin.* **55** 6387 (in Chinese)

[7] Tian Y, Li W, Chen J, Liu L, Liu G, Tkachuk A, Tian J, Xiong Y, Gelb J, Hsu G *et al.* 2008 *Rev. Sci. Instrum.* **79** 103708

[8] Shi S M, Chen R C, Xue Y L, Ren Y Q, Du G H, Deng B, Xie H L and Xiao T Q 2008 *Acta Phys. Sin.* **57** 6319 (in Chinese)

[9] Zhu P, Zhang K, Wang Z, Liu Y, Liu X, Wu Z, McDonald S, Marone F and Stampanoni M 2010 *Proc. Natl. Acad. Sci. USA* **107** 13576

[10] Xue Y L, Xiao T Q, Wu L H, Chen C, Guo R Y, Du G H, Xie H L, Deng B, Ren Y Q and Xu H J 2010 *Acta Phys. Sin.* **59** 5496 (in Chinese)

[11] Bonse U and Hart M 1965 *Appl. Phys. Lett.* **6** 155

[12] Liu X, Guo J C and Niu H B 2010 *Chin. Phys.* B **19** 070701

[13] Gerchberg R W and Saxton W O 1972 *Optik* **35** 237

[14] Fienup J R 1978 *Opt. Lett.* **3** 27

[15] Miao J, Charalambous P, Kirz J and Sayre D 1999 *Nature* **400** 342

[16] Zhou G Z, Tong Y J, Chen C, Ren Y Q, Wang Y D and Xiao T Q 2011 *Acta Phys. Sin.* **60** 028701 (in Chinese)

[17] Zhou G Z, Wang Y D, Ren Y Q, Chen C, Ye L L and Xiao T Q 2012 *Acta Phys. Sin.* **61** 018701 (in Chinese)

[18] Williams G J, Pfeifer M A, Vartanyants I A and Robinson I K 2003 *Phys. Rev. Lett.* **90** 175501

[19] Xiao X and Shen Q 2005 *Phys. Rev.* B **72** 33103

[20] Zhang F and Rodenburg J 2010 *Phys. Rev.* B **82** 121104

[21] Chen C C, Miao J, Wang C W and Lee T K 2007 *Phys. Rev.* B **76** 064113

[22] Li E, Liu Y, Liu X, Zhang K, Wang Z, Hong Y, Yuan Q, Huang W, Marcelli A, Zhu P and Wu Z 2008 *J. Opt. Soc. Am.* A **25** 2651

[23] Cheng J and Han S 1999 *Opt. Commun.* **172** 17

[24] Cheng J and Han S 1999 *Opt. Lett.* **24** 175

[25] Li E, Hwu Y, Chien D, Wang C L and Margaritondo G 2011 *J. Opt.* **13** 035712

[26] Teague M R 1982 *J. Opt. Soc. Am.* **72** 1199

[27] Gureyev T, Mayo S, Wilkins S, Paganin D and Stevenson A 2001 *Phys. Rev. Lett.* **86** 5827

[28] Yu B, Peng X, Tian J and Niu H 2005 *Acta Phys. Sin.* **54** 2034 (in Chinese)

[29] Zhang D, Li Z, Huang Z F, Yu A M and Sha W 2006 *Chin. Phys.* **15** 1731

[30] Liu L X, Du G H, Wen H, Xie H L and Xiao T Q 2007 *Acta Phys. Sin.* **56** 4556 (in Chinese)

[31] Li C, Li Z, Li C Q and Yu A M 2007 *Chin. Phys. Lett.* **24** 2823

[32] Nugent K A, Peele A G, Chapman H N and Mancuso A 2003 *Phys. Rev. Lett.* **91** 203902

[33] Gureyev T, Pogany A, Paganin D and Wilkins S 2004 *Opt. Commun.* **231** 53

[34] Cloetens P, Ludwig W, Baruchel J, Van Dyck D, Van Landuyt J, Guigay J and Schlenker M 1999 *Appl. Phys. Lett.* **75** 2912

[35] Allen L and Oxley M 2001 *Opt. Commun.* **199** 65

[36] Allen L J, Faulkner H M L, Nugent K A, Oxley M P and Paganin D 2001 *Phys. Rev.* E **63** 37602

[37] Zhang F, Pedrini G and Osten W 2007 *Phys. Rev.* A **75** 043805

[38] Liu Y J, Chen B, Li E R, Wang J Y, Marcelli A, Wilkins S W, Ming H, Tian Y C, Nugent K A, Zhu P P and Wu Z Y 2008 *Phys. Rev.* A **78** 023817

[39] Liu Y, Andrews J C, Wang J, Meirer F, Zhu P, Wu Z and Pianetta P 2011 *Opt. Express* **19** 540

[40] Song C, Ramunno-Johnson D, Nishino Y, Kohmura Y, Ishikawa T, Chen C, Lee T and Miao J 2007 *Phys. Rev.* B **75** 12102